PROCEEDINGS OF SCIENCE

Four tops, SM and BSM by ATLAS and CMS, including EFT interpretations

Sandeep Bhowmik[a,*]
on behalf of the ATLAS and CMS Collaborations

[a] *Instituto de Física de Cantabria (CSIC - Universidad de Cantabria), Av. de los Castros, 39005 Santander, Spain*

E-mail: sandeep.bhowmik@cern.ch

This article presents the observation of four-top-quark ($t\bar{t}t\bar{t}$) production in proton-proton collisions by the ATLAS and CMS experiments at the CERN LHC. The analysis is performed using data samples collected by both experiments separately at a center-of-mass energy of 13 TeV during 2016-2018 and corresponding to an integrated luminosity of 140 fb^{-1} and 138 fb^{-1} by the ATLAS and CMS Collaborations respectively. Events containing two leptons with the same charge or at least three leptons (electrons or muons) are selected. Event kinematics are used to separate signal from background through a multivariate discriminant, and dedicated control regions are used to constrain the dominant backgrounds. The observed (expected) significance of the measured $t\bar{t}t\bar{t}$ signal with respect to the standard model background-only hypothesis is 6.1 (4.3) standard deviations by the ATLAS and 5.6 (4.9) standard deviations by CMS experiment. The $t\bar{t}t\bar{t}$ production cross section is measured to be $22.5^{+6.6}_{-5.5}$ fb and $17.7^{+4.4}_{-4.0}$ fb by the ATLAS and CMS experiment respectively, in agreement with the available standard model predictions. The limits are set by the ATLAS experiment on the three-top-quark production cross section, being an irreducible background not measured previously, and constraints are obtained the top-Higgs Yukawa coupling and Wilson coeficients corresponding to the effective field theory operators sensitive to the $t\bar{t}t\bar{t}$ production.

16th International Conference on Heavy Quarks and Leptons (HQL2023)
28 November-2 December 2023
TIFR, Mumbai, Maharashtra, India

[*]Speaker

PoS(HQL2023)052

1. Introduction

The top quark is the heaviest elementary particle in the Standard Model (SM) and has a strong connection to the Higgs boson as well as potentially new particles in various theories beyond the SM (BSM). It is therefore relevant to study rare processes involving the top quark, such as the production of four top quarks ($\mathrm{t\bar{t}t\bar{t}}$), which is predicted by the SM and has been observed for the first time [1, 2] by the ATLAS [3] and CMS [4] Collaborations at the CERN LHC.

While the production occurs predominantly through the strong interaction [5–7], nonnegligible contributions arise also from electroweak (EW) processes [8–10]. Example leading-order (LO) Feynman diagrams are shown in Figure 1. The SM cross section is calculated at next-to-LO (NLO) in quantum chromodynamics (QCD) and EW theory, including soft-gluon emission corrections at next-to-leading logarithmic accuracy, to be $13.4^{+1.0}_{-1.8}$ fb at $\sqrt{s} = 13$ TeV [10]. The quoted uncertainty is due to scale variations and parton distribution functions (PDFs).

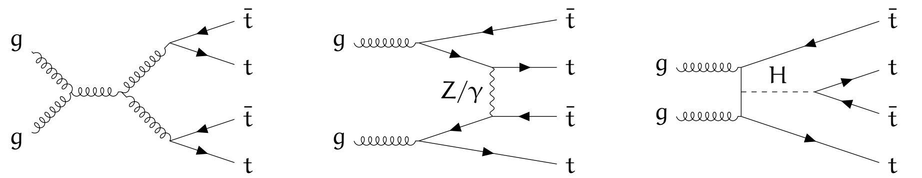

Figure 1: Examples of Feynman diagrams that provide important contributions to $\mathrm{t\bar{t}t\bar{t}}$ production. The first diagram (left) involves only the strong interaction, while the other two involve both strong and electroweak interactions with the exchange of a Z boson or virtual photon (middle), or a Higgs boson (right) [2].

The $\mathrm{t\bar{t}t\bar{t}}$ cross section could be enhanced in many BSM models, including gluino pair production in supersymmetric theories [11, 12], scalar-gluon pair production [13, 14], the associated production of a heavy scalar or pseudoscalar boson with a top-quark pair in two-Higgs-doublet models [15–17], or in top-quark-compositeness models [18]. Additionally, the $\mathrm{t\bar{t}t\bar{t}}$ cross section is sensitive to the strength of the top-quark Yukawa coupling, and its charge conjugation and parity (CP) properties [19, 20]. It is also sensitive to various four-fermion interactions [21–24] and the Higgs oblique parameter [25] in the context of an effective field theory (EFT) framework.

The $\mathrm{t\bar{t}t\bar{t}}$ process results in various final states depending on the top quark decays. These final states are classified based on the number of electrons or muons produced in the top quark decays, including those originating from subsequent leptonic τ decays. This article focuses on two types of events: those with exactly two same-signed isolated leptons (2LSS) and those with at least three isolated leptons (3L). In the SM, 7% and 5% of the produced $\mathrm{t\bar{t}t\bar{t}}$ events result in 2LSS and 3L final states, respectively. While these channels are relatively rare final states, they are advantageous due to low levels of background. The $\mathrm{t\bar{t}t\bar{t}}$ topology is also characterised by a high light-jet and b-jet multiplicity and a large rest mass of the event, amounting to about 700 GeV.

The ATLAS and CMS experiments reported evidence for $\mathrm{t\bar{t}t\bar{t}}$ production in 13 TeV pp collisions at the LHC. The ATLAS result combines two analyses using 139 fb^{-1} at $\sqrt{s} = 13$ TeV: one in the 2LSS/3L channel [26] and the other in the channel comprising events with one lepton or two leptons with opposite electric charge. This combination results in a measured cross-section of 24^{+7}_{-6} fb, corresponding to an observed (expected) signal significance of 4.7 (2.6) standard deviations (SDs)

PoS(HQL2023)052

over the background-only predictions [27]. The CMS result is from a combination of several measurements based on 138 fb^{-1} at $\sqrt{s}$ = 13 TeV, in the channels with zero, one and two electrons or muons of opposite charge and the 2LSS/3L channel, yielding an observed (expected) significance of 4.0 (3.2) SDs [28]. The $t\bar{t}t\bar{t}$ cross section measured by the CMS Collaboration is 17±5 fb.

2. Analysis procedure

Monte Carlo (MC) simulated samples are used to model different signal and background processes. Events were selected using single-lepton, dilepton or trilepton triggers with variable electron and muon transverse momentum thresholds, and various identification and isolation criteria depending on the lepton flavour and data-taking period with an aim of maximizing the acceptance for $t\bar{t}t\bar{t}$ decays while simultaneously rejecting the large backgrounds. Signal regions (SRs) and control regions (CRs) are defined using events in which all leptons pass the tight ID criteria, whereas events with at least one loose lepton are used as a sideband for the nonprompt-lepton background estimation. The background composition of the SR is largely dominated by the production of top-quark pairs in association with bosons. The study of the ATLAS experiment has used a multivariate discriminant built with a Graph Neural Network (GNN) [29] to separate the $t\bar{t}t\bar{t}$ signal from the background. To enhance the separation between signal events and those from different background processes, the CMS experiment employs multiclassification boosted decision trees (BDTs). The GNN training is performed for events passing the SR requirements. The LO $t\bar{t}t\bar{t}$ simulated signal sample is used in the training. The MC simulated samples, corresponding to all background components, represent the background in the training. The GNN discriminant is chosen as the observable of the analysis to extract the $t\bar{t}t\bar{t}$ signal. Figure 2 shows the distribution of the GNN score in the SR. Similarly, the CMS experiment has used simulated event samples of $t\bar{t}t\bar{t}$, $t\bar{t}Z$, $t\bar{t}W$, $t\bar{t}H$, and $t\bar{t}$ production in the training. The rate of the $t\bar{t}t\bar{t}$ signal is extracted through a binned maximum-likelihood (ML) fit to the distributions in the output of GNN (for ATLAS) and BDT (for CMS) classifiers. The lepton misidentification and electron charge misidentification backgrounds are both determined from data, while electron conversions and irreducible backgrounds are modeled using MC simulation. The ATLAS experiment has estimated the $t\bar{t}W$ background also from data. The multiple sources of systematic uncertainty are considered which affect the predicted event yields, the distributions in the output of the BDT classifiers, or both.

Ref. [1] presents a re-analysis of the 140 fb^{-1} data set at $\sqrt{s}$ = 13 TeV in the 2LSS/3L channel with the ATLAS detector and supersedes the result of Ref. [26]. Compared to the previous result that showed evidence for $t\bar{t}t\bar{t}$ production [26], this new measurement brings several improvements: an optimised selection with lower thresholds on the leptons' and jets' transverse momenta; improved b-jet identification; a new data-driven estimation of the $t\bar{t}W$+jets background, one of the main backgrounds in this channel; a revised set of systematic uncertainties; an improved treatment of the $t\bar{t}t$ background and a more powerful multivariate discriminant to separate the signal from background.

Ref. [2] presents a search for $t\bar{t}t\bar{t}$ production in events with two same-sign, three, or four leptons, using pp collision data recorded by the CMS experiment in 2016–2018 and corresponding to an integrated luminosity of 138 fb^{-1}. This measurement supersedes the results from Ref. [30] that analyzed events with two same-sign or at least three leptons selected from the same data set and found 2.6 (2.7) SDs of observed (expected) significance for $\mathrm{t\bar{t}t\bar{t}}$ production. Notable improvements, discussed in Ref. [2], are achieved in the lepton identification and the tagging of jets originating from the hadronization of bottom quarks, as well as from a revised analysis strategy for the discrimination between signal and background processes based on the application of machine learning techniques. The aforementioned improvements increase the sensitivity of the analysis and allow for the observation of the $\mathrm{t\bar{t}t\bar{t}}$ production process with a statistical significance above five SDs.

3. Results

A maximum-likelihood fit is performed to the GNN score distribution in the SR and to different distributions in the CRs to constrain the dominant backgrounds. Figure 2 shows the distribution of the GNN score in the SR before and after performing the fit by the ATLAS experiment. A good agreement is observed between data and the prediction after the fit. The measured $\mathrm{t\bar{t}t\bar{t}}$ production cross section is:

$$\sigma_{\mathrm{t\bar{t}t\bar{t}}} = 22.5^{+4.7}_{-4.3}(\mathrm{stat})^{+4.6}_{-3.4}(\mathrm{syst})\mathrm{fb} = 22.5^{+6.6}_{-5.5}\mathrm{fb}. \quad (1)$$

The measured cross section is consistent within 1.7 SDs with the SM prediction of Ref. [10].

The measured cross sections of the $\mathrm{t\bar{t}t\bar{t}}$ signal process is extracted from a simultaneous binned profile likelihood fit to the data in the SRs and CRs by the CMS experiment. Figure 3 shows the yields in the SR $\mathrm{t\bar{t}t\bar{t}}$ classes after the fit. The results when fitting each channel on its own are summarized in Figure 4, with the largest sensitivity provided by the 2l channel. The cross section of $\mathrm{t\bar{t}t\bar{t}}$ production is measured to be

$$\sigma_{\mathrm{t\bar{t}t\bar{t}}} = 17.7^{+3.7}_{-3.5}(\mathrm{stat})^{+2.3}_{-1.9}(\mathrm{syst})\mathrm{fb} = 17.7^{+4.4}_{-4.0}\mathrm{fb}. \quad (2)$$

This result is in agreement with the SM prediction of $13.4^{+1.0}_{-1.8}$ fb [10] at the level of 1.0 SDs, when uncertainties of both prediction and measurement are taken into account.

The probability for the background-only hypothesis to result in a signal-like excess at least as large as seen in data is derived with the profile-likelihood ratio following the procedure described in Ref. [31]. From this, the significance of the observed signal is found to be 6.1 SDs by the ATLAS experiment and 5.6 SDs by the CMS experiment. Using the SM cross section of $13.4^{+1.0}_{-1.8}$ fb from Ref. [10], the expected significance would be 4.7 SDs by ATLAS and 4.9 SDs by CMS.

3.1 Systematic uncertainties

The dominant experimental uncertainties arise from the measurement of b-tagging efficiencies and mis-tagging rates. Uncertainties in the calibration of the jet energy scale and resolution play a subleading role among the experimental uncertainties. Other uncertainties have minor impacts on the measurements. Uncertainties in the modelling of SM $\mathrm{t\bar{t}t\bar{t}}$ production have the dominant impact on the measurements. The dominant uncertainty in the background predictions arises from the modelling of $\mathrm{t\bar{t}W}$, $\mathrm{t\bar{t}H}$ and $\mathrm{t\bar{t}Z}/\gamma^{*}$ events. The uncertainty in the predicted cross-sections of background processes have minor impact on the measurements. Uncertainties in the estimate of fake/non-prompt backgrounds have minor impact.

PoS(HQL2023)052

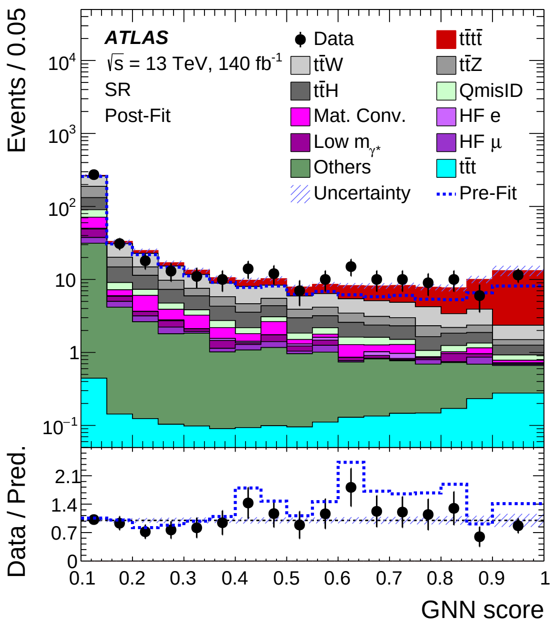

Figure 2: Comparison between data and predictions after a fit to data for the GNN distribution in the SR. The first bin contains underflow events. The ratio of the data to the total post-fit prediction is shown in the lower panel. The dashed blue lines show the pre-fit prediction in the upper panel and the ratio of the data to the total pre-fit prediction in the lower panel. The shaded band represents the total post-fit uncertainty in the prediction [1].

4. Interpretations

Limits at 95% CL intervals are also obtained by the ATLAS experiment on the top-quark Yukawa coupling, on EFT operators that parametrize BSM $t\bar{t}t\bar{t}$ production, and on a Higgs oblique parameter.

4.1 Limits on the top-quark Yukawa coupling

The $t\bar{t}t\bar{t}$ cross section can be parameterised as a function of two parameters: the top Yukawa coupling strength modifier κ_t and the CP-mixing angle α [20, 32]. The $t\bar{t}t\bar{t}$ and $t\bar{t}H$ yields in each bin of the GNN distribution are parameterised as a function of κ_t and α. The observed (expected) 95% CL limits are shown in Figure 5 in the two-dimensional parameter space $(|\kappa_t \cos(\alpha)|, |\kappa_t \sin(\alpha)|)$. Fixing the top-quark Yukawa coupling to be CP-even only (i.e. $\alpha = 0$), the following observed (expected) limits are extracted: $|\kappa_t| < 1.8$ (1.6).

4.2 Limits on EFT operators and the Higgs oblique parameter

Within the EFT framework, the $t\bar{t}t\bar{t}$ process is sensitive to four heavy-flavour fermion operators O^1_{tt}, O^1_{QQ}, O^1_{Qt} and O^8_{Qt} which can probe the BSM models that enhance interactions between the third-generation quarks [22]. The $t\bar{t}t\bar{t}$ production cross section can be approximated by:

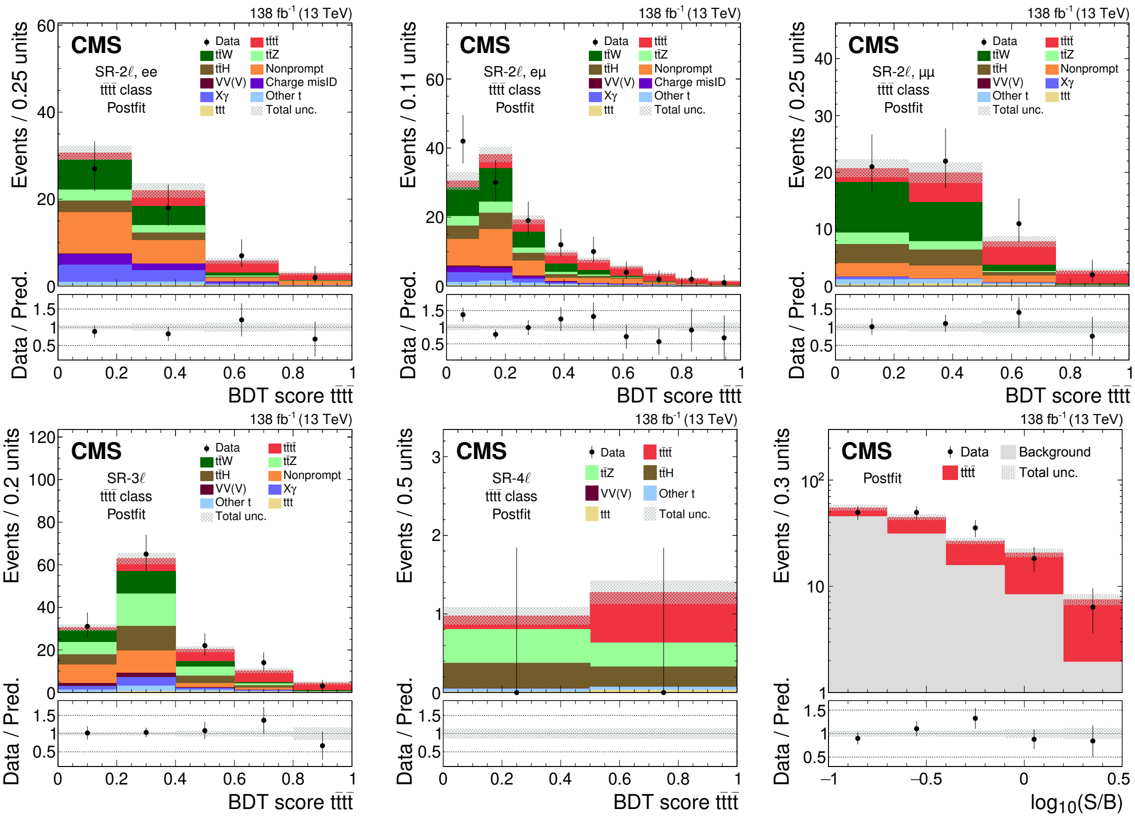

Figure 3: Comparison of the number of observed (points) and predicted (colored histograms) events in the BDT score $t\bar{t}t\bar{t}$ in the $t\bar{t}t\bar{t}$ classes of SR-2l, shown for the ee (upper left), eμ (upper middle), and $\mu\mu$ (upper right) categories, of SR-3l (lower left) and of SR-4l (lower middle). Additionally, the comparison is shown for all SRs combined as a function of $\log_{10}$(S/B) (lower right), where S and B are evaluated for each bin of the fitted distributions as the predicted signal and background yields before the fit to data. Bins with $\log_{10}$(S/B) < -1 are not included, and bins with $\log_{10}$(S/B) > 0.5 are included in the last bin. The vertical bars on the points represent the statistical uncertainties in the data, and the hatched bands the total uncertainty in the predictions. The signal and background yields are shown with their best fit normalizations from the simultaneous fit to the data ("postfit") [2].

$$\sigma_{t\bar{t}t} = \sigma^{\mathrm{SM}}_{t\bar{t}t} + \frac{1}{\Lambda^2}\sum_{\mathrm{i}} \mathrm{C_i}\sigma^{(1)}_{\mathrm{i}} + \frac{1}{\Lambda^4}\sum_{\mathrm{i}\le \mathrm{j}} \mathrm{C_i C_j}\sigma^{(2)}_{\mathrm{i,j}} \tag{3}$$

where Λ is the energy scale, $\mathrm{C_i}$ denotes the coupling parameters of the four heavy-flavour fermion operators, $\mathrm{C_i}\sigma^{(1)}_{\mathrm{i}}$ is the linear term that represents the interference of dimension-6 operators with SM operators, and $\mathrm{C_i C_j}\sigma^{(2)}_{\mathrm{i,j}}$ is the quadratic term that also includes the interference between different EFT operators. The 95% CL intervals on the EFT parameters are extracted by parameterising the $t\bar{t}t$ yield in each bin of the GNN score distribution as a quadratic function of the coefficient of the corresponding EFT operator ($\mathrm{C_i}/\Lambda^2$) and then by performing the fit to data. The fit is carried out assuming that only one operator contributes to the $t\bar{t}t$ cross section, while the coefficients of the other three operators are fixed to the SM value of zero. The observed 95% CL

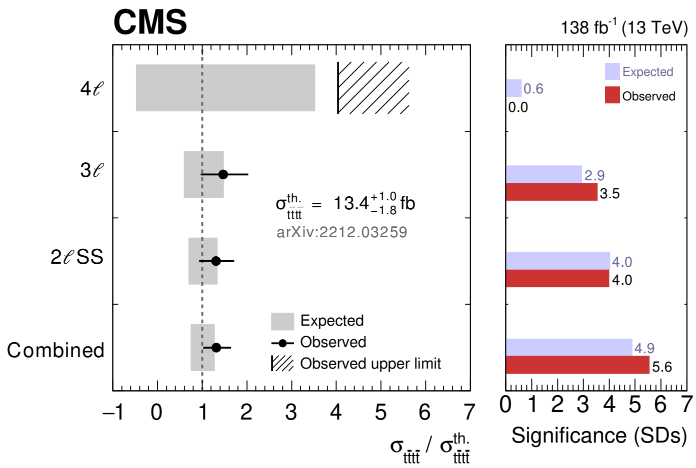

Figure 4: Comparison of fit results in the channels individually and in their combination. The left panel shows the values of the measured cross section relative to the SM prediction from Ref. [10] , where the displayed uncertainty does not include the uncertainty in the SM prediction. For the 4l channel, no events were observed in the $t\bar{t}t\bar{t}$-enriched bins, and an upper limit at 95% confidence level is quoted. The right panel shows the expected and observed significance, with the printed values rounded to the first decimal [2].

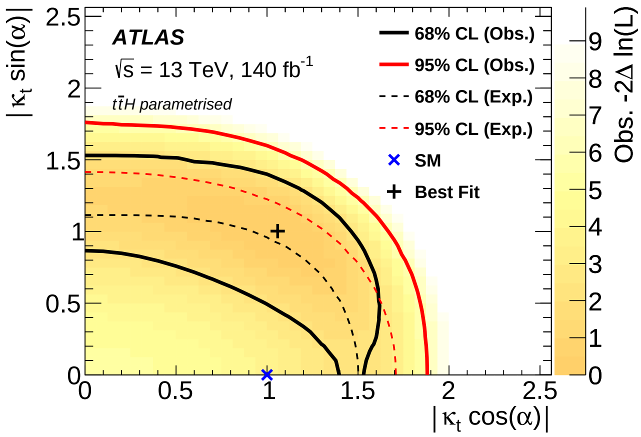

Figure 5: Two-dimensional negative log-likelihood contours for $|\kappa_t \cos(\alpha)|$ versus $|\kappa_t \sin(\alpha)|$ at 68% and 95%, where κ_t is the top-Higgs Yukawa coupling strength parameter and α is the mixing angle between the CP-even and CP-odd components. The gradient-shaded area represents the observed likelihood value as a function of κ_t and α. Both the $t\bar{t}t\bar{t}$ signal and $t\bar{t}H$ background yields in each fitted bin are parameterised as a function of κ_t and α. The blue plus shows the SM expectation, while the black cross shows the best fit value [1].

intervals on the coefficients ($|C_i/\Lambda^2|$) of O^1_{QQ}, O^1_{Qt}, O^1_{tt}, and O^8_{Qt} are [-3.5, 4.1], [-3.5, 3.0], [-1.7, 1.9], and [-6.2, 6.9] TeV^{-2}, respectively.

The Higgs oblique ($\hat{H}$) parameter affects the off-shell Higgs interaction, and thus the $t\bar{t}t\bar{t}$ cross section, as well as processes involving a Higgs boson, in particular $t\bar{t}H$ production, which is a significant background to the $t\bar{t}t\bar{t}$ measurement [25]. A limit on $\hat{H}$ is extracted from the likelihood scans shown on Figure 6. The observed (expected) upper limit on the $\hat{\mathrm{H}}$ value is 0.20 (0.12) at 95% CL.

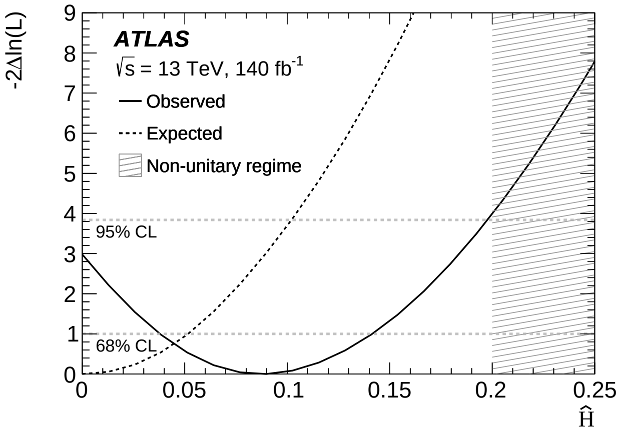

Figure 6: The negative log-likelihood values as a function of the Higgs oblique parameter $\hat{\mathrm{H}}$. The solid curve represents the observed likelihood while the dashed curve corresponds to the expected one. The dashed regions shows the non-unitary regime. [1].

5. Conclusion

Four-top-quark production is observed with a significance of 6.1 standard deviations by the ATLAS experiment and 5.6 standard deviations by CMS experiment with respect to the background-only hypothesis. The corresponding expected significances are 4.7 and 4.9 standard deviations. The measured $t\bar{t}t\bar{t}$ production cross section is $22.5^{+6.6}_{-5.5}$ fb and $17.7^{+4.4}_{-4.0}$ fb by ATLAS and CMS respectively, in agreement with the standard model predictions.

The results of the ATLAS experiment are used to set limits on several new physics scenarios. Constraints on the CP properties of the top-quark Yukawa coupling are obtained in the form of limits in the two-dimensional parameter space ($|\kappa_t \cos(\alpha)|$, $|\kappa_t \sin(\alpha)|$). Assuming a pure CP-even coupling ($\alpha = 0$), the observed upper limit on $|\kappa_t| = |y_t/y_t^{SM}|$ at 95% CL is 1.8. Constraints at 95% CL are obtained on the four dimension-6 heavy-flavour fermion operators. Assuming one operator taking effect at a time, the observed constraints on the coefficients (C_i/Λ^2) of O^1_{tt}, O^1_{QQ}, O^1_{Qt}, and Q^8_{Qt} are [-3.5, 4.1], [-3.5, 3.0], [-1.7, 1.9], and [-6.2, 6.9] TeV^{-2}, respectively. An observed upper limit at 95% CL of 0.20 is obtained for the Higgs oblique parameter that coincides with the largest value that preserves unitarity for the perturbative theory.

References

[1] ATLAS Collaboration, *"Observation of four-top-quark production in the multilepton final state with the ATLAS detector"*, Eur. Phys. J. C 83 (2023) 496, doi: 10.1140/epjc/s10052-023-11573-0, arXiv:2303.15061v2

PoS(HQL2023)052

[2] CMS Collaboration, *"Observation of four top quark production in proton-proton collisions at $\sqrt{s}$ = 13 TeV"*, Phys. Lett. B 847 (2023) 138290, doi: 10.1016/j.physletb.2023.138290, arXiv:2305.13439v1

[3] ATLAS Collaboration, *"The ATLAS experiment at the CERN Large Hadron Collider"*, JINST 3 (2008) S08003, doi:10.1088/1748-0221/3/08/S08003.

[4] CMS Collaboration, *"The CMS experiment at the CERN LHC"*, JINST 3 (2008) S08004, doi:10.1088/1748-0221/3/08/S08004.

[5] G. Bevilacqua and M. Worek, *"Constraining BSM physics at the LHC: Four top final states with NLO accuracy in perturbative QCD"*, JHEP 07 (2012) 111, doi:10.1007/JHEP07(2012)111, arXiv:1206.3064.

[6] J. Alwall et al., *"The automated computation of tree-level and next-to-leading order differential cross sections, and their matching to parton shower simulations"*, JHEP 07 (2014) 079, doi:10.1007/JHEP07(2014)079, arXiv:1405.0301.

[7] F. Maltoni, D. Pagani, and I. Tsinikos, *"Associated production of a top-quark pair with vector bosons at NLO in QCD: impact on* $\mathrm{t\bar{t}H}$ *searches at the LHC"*, JHEP 02 (2016) 113, doi:10.1007/JHEP02(2016)113, arXiv:1507.05640.

[8] R. Frederix, D. Pagani, and M. Zaro, *"Large NLO corrections in* $\mathrm{t\bar{t}W^{\pm}}$ *and* $\mathrm{t\bar{t}t\bar{t}}$ *hadroproduction from supposedly subleading EW contributions"*, JHEP 02 (2018) 031, doi:10.1007/JHEP02(2018)031, arXiv:1711.02116.

[9] T. Jezo and M. Kraus, *"Hadroproduction of four top quarks in the POWHEG BOX"*, Phys. Rev. D 105 (2022) 114024, doi:10.1103/PhysRevD.105.114024, arXiv:2110.15159.

[10] M. van Beekveld, A. Kulesza, and L. Moreno Valero, *"Threshold resummation for the production of four top quarks at the LHC"*, 2022. arXiv:2212.03259.

[11] H. P. Nilles, *"Supersymmetry, supergravity and particle physics"*, Phys. Rept. 110 (1984) 1.

[12] G. R. Farrar and P. Fayet, *"Phenomenology of the production, decay, and detection of new hadronic states associated with supersymmetry"*, Phys. Lett. B 76 (1978) 575.

[13] T. Plehn and T. M. P. Tait, *"Seeking sgluons"*, J. Phys. G 36 (2009) 075001, arXiv: 0810.3919

[14] S. Calvet, B. Fuks, P. Gris and L. Valéry, *"Searching for sgluons in multitop events at a center-of-mass energy of 8 TeV"*, JHEP 04 (2013) 043, arXiv: 1212.3360

[15] D. Dicus, A. Stange and S. Willenbrock, *"Higgs decay to top quarks at hadron colliders"*, Phys. Lett. B 333 (1994) 126, arXiv: hep-ph/9404359.

[16] N. Craig, F. D'Eramo, P. Draper, S. Thomas and H. Zhang, *"The hunt for the rest of the Higgs bosons"*, JHEP 06 (2015) 137, arXiv: 1504.04630.

PoS(HQL2023)052

[17] N. Craig, J. Hajer, Y.-Y. Li, T. Liu and H. Zhang, *"Heavy Higgs bosons at low tan β: from the LHC to 100 TeV"*, JHEP 01 (2017) 018, arXiv: 1605.08744

[18] A. Pomarol and J. Serra, *"Top quark compositeness: Feasibility and implications"*, Phys. Rev. D 78 (7 2008) 074026, arXiv: 0806.3247

[19] Q.-H. Cao, S.-L. Chen and Y. Liu, *"Probing Higgs width and top quark Yukawa coupling from* $\mathrm{t\bar{t}H}$ *and* $\mathrm{t\bar{t}t\bar{t}}$ *productions"*, Phys. Rev. D 95 (2017) 053004, arXiv: 1602.01934

[20] Q.-H. Cao, S.-L. Chen, Y. Liu, R. Zhang and Y. Zhang, *"Limiting top quark-Higgs boson interaction and Higgs-boson width from multitop productions"*, Phys. Rev. D 99 (2019) 113003, arXiv: 1901.04567

[21] C. Degrande, J.-M. Gerard, C. Grojean, F. Maltoni and G. Servant, *"Non-resonant new physics in top pair production at hadron colliders"*, JHEP 03 (2011) 125, arXiv: 1010.6304

[22] C. Zhang, *"Constraining $qqtt$ operators from four-top production: a case for enhanced EFT sensitivity"*, Chin. Phys. C 42 (2018) 023104, arXiv: 1708.05928

[23] G. Banelli, E. Salvioni, J. Serra, T. Theil and A. Weiler, *"The present and future of four top operators"*, JHEP 02 (2021) 043, arXiv: 2010.05915

[24] R. Aoude, H. El Faham, F. Maltoni and E. Vryonidou, *"Complete SMEFT predictions for four top quark production at hadron colliders"*, JHEP 10 (2022) 163, arXiv: 2208.04962

[25] C. Englert, G. F. Giudice, A. Greljo and M. Mccullough, *"The $\hat{H}$-parameter: an oblique Higgs view"*, JHEP 09 (2019) 041, arXiv: 1903.07725

[26] ATLAS Collaboration, *"Evidence for* $\mathrm{t\bar{t}t\bar{t}}$ *production in the multilepton final state in proton-proton collisions at $\sqrt{s}$ = 13TeV with the ATLAS detector"*, Eur. Phys. J. C 80 (2020) 1085, arXiv: 2007.14858

[27] ATLAS Collaboration, *"Measurement of the* $\mathrm{t\bar{t}t\bar{t}}$ *production cross section in pp collisions at $\sqrt{s}$ = 13 TeV with the ATLAS detector"*, JHEP 11 (2021) 118, arXiv: 2106.11683

[28] CMS Collaboration, *"Evidence for four-top quark production in proton-proton collisions at $\sqrt{s}$ = 13 TeV"*, (2023), arXiv: 2303.03864

[29] P. W. Battaglia et al., *"Relational inductive biases, deep learning, and graph networks"*, (2018), arXiv: 1806.01261.

[30] CMS Collaboration, *"Search for production of four top quarks in final states with same-sign or multiple leptons in proton-proton collisions at $\sqrt{s}$ = 13 TeV"*, Eur. Phys. J. C 80 (2020) 75, doi:10.1140/epjc/s10052-019-7593-7, arXiv:1908.06463.

[31] G. Cowan, K. Cranmer, E. Gross, and O. Vitells, *"Asymptotic formulae for likelihood-based tests of new physics"*, Eur. Phys. J. C 71 (2011) 1554

[32] ATLAS Collaboration, *"CP Properties of Higgs Boson Interactions with Top Quarks in the* $\mathrm{t\bar{t}H}$ *and* tH *Processes Using* $\mathrm{H} \rightarrow \gamma\gamma$ *with the ATLAS Detector"*, Phys. Rev. Lett. 125 (2020) 061802, arXiv: 2004.04545